

Supporting Information for

Temperature Effects on the Nanoindentation Characterization of Stiffness

Gradients in Confined Polymers

Jake Song, Ridvan Kahraman, David W. Collinson, Wenjie Xia,

L. Catherine Brinson*, Sinan Keten*

*Corresponding Authors: s-keten@northwestern.edu, cate.brinson@duke.edu

Sections

1. Tip-polymer adhesion effects on characterization of the mechanical interphase	2
2. Vibrational force constant calculations	2
3. Force field for the poly(methyl methacrylate) coarse-grained model employed in the study	3
4. Figures	4
5. References	9

1. Tip-polymer adhesion effects on characterization of the mechanical interphase

Tip-polymer attraction is a very relevant problem in experimental indentation studies, and requires addressing through different contact mechanics methods such as the Johnson-Kendall-Roberts model, the Derjaguin-Muller-Toporov model, or the Maugis-Dugdale model and their variants. In our simulation studies however, we have found that the attraction plays a minor role in determining the stiffness gradient in the polymer nanocomposite. Despite creating a much larger contact area (Fig. S1A), an increase in the tip-polymer attraction via the interaction strength parameter ε_i plays a very small role in the stiffness response of the film i.e. the slope (Fig. S1B) and the overall stress field response (Fig. S1C - see Section S5 for calculation protocol). As a testimony to this, we find that obtaining local stiffness profiles using both $\varepsilon_i = 0.1$ kcal/mol and $\varepsilon_i = 0.5$ kcal/mol yield essentially the identical interphase length-scale ξ_{int} (Fig. S1A). We therefore maintain the use of $\varepsilon_i = 0.1$ kcal/mol throughout the rest of the text.

2. Vibrational force constant calculations

As indentation is a contact method that relies on the stress field for mechanical property measurements, the range of the stress field will play an important role in the measured stiffness, especially in confined systems due to the substrate effect.¹ Recent studies have discussed the effect of local caging stiffness on the stress propagation and substrate effect in glassy polymers.¹⁻³ This local caging stiffness can be approximated by the vibrational force constant f , which is related to the picosecond mean-squared displacement $\langle u^2 \rangle$ of the polymer:

$$f \sim \frac{k_B T}{\langle u^2 \rangle} \quad (\text{S1})$$

$\langle u^2 \rangle$ increases linearly with temperature in glassy regimes before increasing non-linearly (Fig. S5) which is attributed to the increased effect of anharmonic vibrations. f for a given polymer was suggested to be inversely related to stress propagation, the size of which is conventionally understood to dictate ξ_{int} .^{1-2, 4} While our results in tracking the segmental $\langle u^2 \rangle$ of PMMA in MD are consistent with this idea in the sense that ξ_{int} is inversely related to f (Fig. 2C), the wide range of viscoelastic states investigated in our simulations above the glass transition brings the effects of stress dissipation and increasing incompressibility into play. Therefore, further explanations for the increase in ξ_{int} with temperature are required.

3. Force field for the poly(methyl methacrylate) coarse-grained model employed in the study

TABLE S1. Coarse-grained force field for poly(methyl methacrylate).⁵

Interaction	Potential Form	Parameters
AA Bond	$U_{bondAA}(l) = k(l - l_0)^2$	$k = 105.0 \text{ kcal/mol} \cdot \text{\AA}^2$, $l_0 = 2.735 \text{ \AA}$
AB Bond Length	$U_{bondAB}(l) = k(l - l_0)^2$	$k = 39.86 \text{ kcal/mol} \cdot \text{\AA}^2$, $l_0 = 3.658 \text{ \AA}$
AAA Angle	$U_{angleAAA}(\theta) = -k_b T \ln \left[a_1 \exp\left(-\frac{\theta - \theta_1}{b_1}\right)^2 + a_2 \exp\left(-\frac{\theta - \theta_2}{b_2}\right)^2 \right]$	$a_1 = 2.294e-2$, $a_2 = 4.367e-3$, $b_1 = 9.493^\circ$, $b_2 = 6.210^\circ$, $\theta_1 = 121.0^\circ$, $\theta_2 = 158.5^\circ$
AAB Angle	$U_{angleAAB}(\theta) = k_2(\theta - \theta_0)^2 + k_3(\theta - \theta_0)^3 + k_4(\theta - \theta_0)^4$	$k_2 = 9.881 \text{ kcal/mol} \cdot \text{rad}^2$, $k_3 = -15.12 \text{ kcal/mol} \cdot \text{rad}^3$, $k_4 = 6.589 \text{ kcal/mol} \cdot \text{rad}^4$, $\theta_0 = 1.690 \text{ rads}$
AAAA Dihedral Angle	$U_{dihedralAAAA}(\phi) = \sum_{k=1}^5 A_k \cos^{k-1}(\phi)$	$A_1 = 4.380 \text{ (kcal/mol)}$, $A_2 = 0.8739 \text{ (kcal/mol)}$, $A_3 = -0.3571 \text{ (kcal/mol)}$, $A_4 = -0.2774 \text{ (kcal/mol)}$, $A_5 = 0.09312 \text{ (kcal/mol)}$
BAAB Dihedral Angle	$U_{dihedralBAAB}(\phi) = \sum_{k=1}^5 A_k \cos^{k-1}(\phi)$	$A_1 = 4.519 \text{ (kcal/mol)}$, $A_2 = -0.8859 \text{ (kcal/mol)}$, $A_3 = -1.692 \text{ (kcal/mol)}$, $A_4 = 0.5625 \text{ (kcal/mol)}$, $A_5 = 0.9562 \text{ (kcal/mol)}$
Non-bonded	$U_{nonbond} = 4\varepsilon \left[\left(\frac{\sigma}{r}\right)^{12} - \left(\frac{\sigma}{r}\right)^6 \right] + S_{LJ}(r)$	$\varepsilon_{AA} = 0.500 \text{ (kcal/mol)}$, $\sigma_{AA} = 5.500 \text{ \AA}$ $\varepsilon_{BB} = 1.500 \text{ (kcal/mol)}$, $\sigma_{BB} = 4.420 \text{ \AA}$

4. Figures

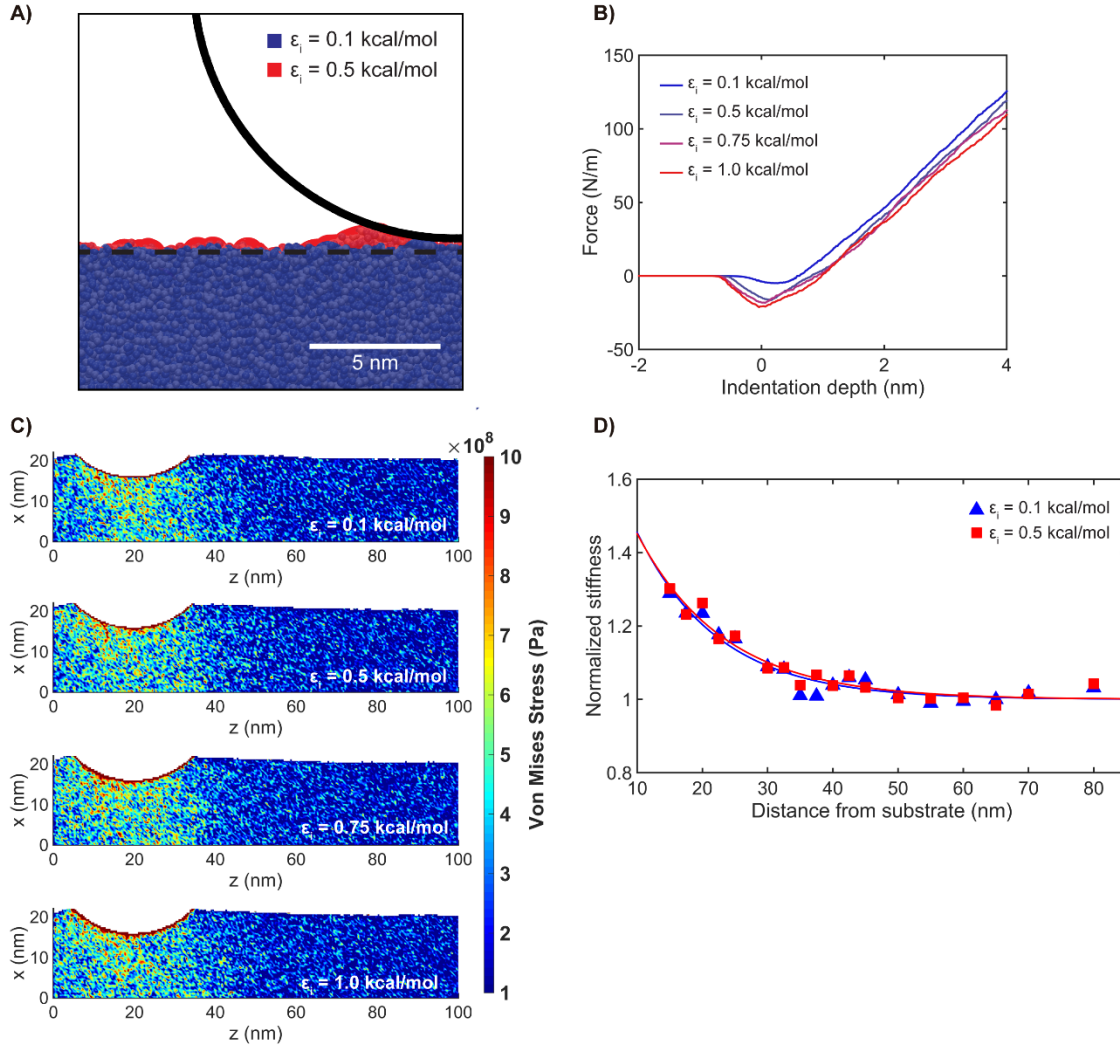


Figure S1. Indentation study with varying tip-polymer interaction strengths ϵ_i . (A)

Adhesion profile of the indenter upon approaching the polymer film during indentation using

different ϵ_i . (B) Force-displacement curves and (C) Von Mises stress fields at $d \sim 5$ nm (see

Section 3 for calculation methods), both obtained from loading the polymer at $z = 20$ nm. All

indentations are performed using $R = 20$ nm. (D) Normalized local stiffness profiles at $T = 300$

K. A single exponential decay function (Eqn. 2, main text) is sufficient for capturing the gradient

profile of both sets of interaction strengths.

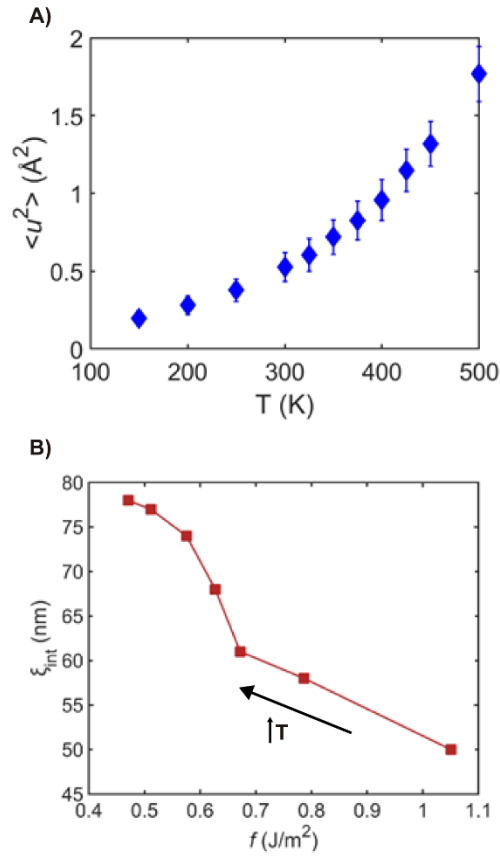


Figure S2. Segmental mean-squared displacement $\langle u^2 \rangle$ and vibrational force constant f as a function of temperature and correlation to the measured ξ_{int} in the CG-PMMA system.

(A) $\langle u^2 \rangle$ increases linearly at lower temperatures before increasing in a non-linear manner. (B) f shows a (negative) linear correlation with ξ_{int} at lower temperatures. This correlation becomes non-linear around the T_g and the ξ_{int} increase becomes proportionally larger.

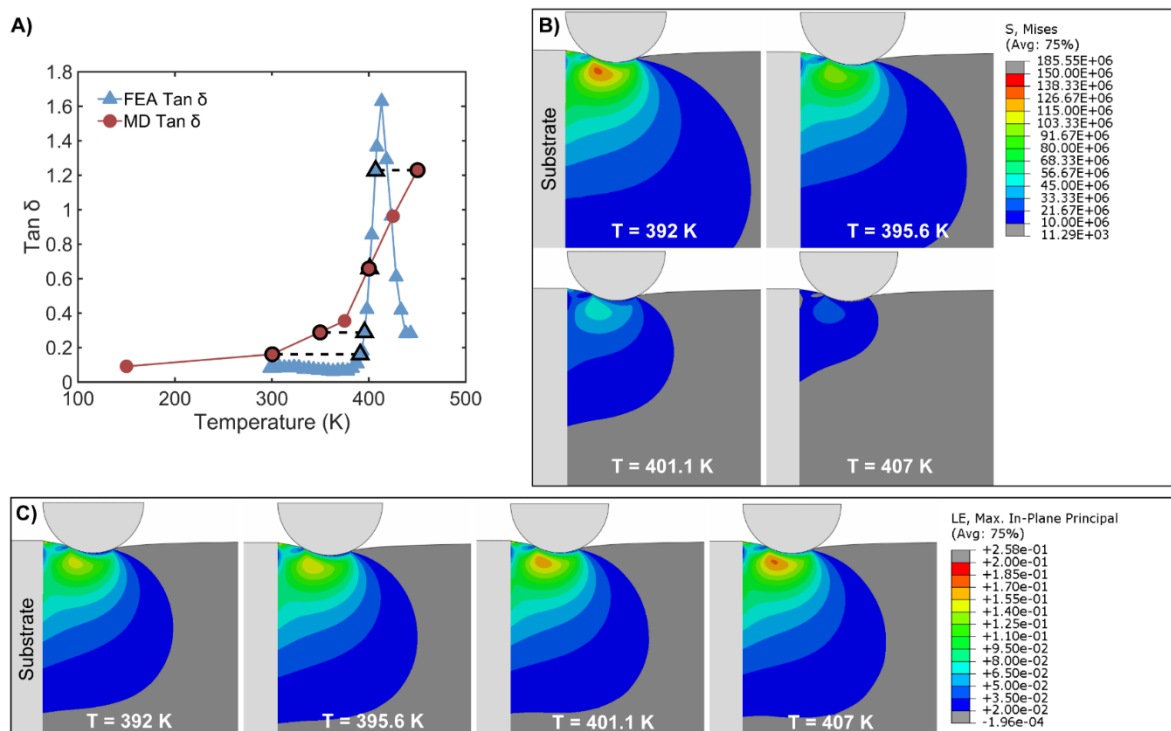


Figure S3. Von Mises stress and strain fields obtained from FEA indentation simulations at varying temperatures. (A) Comparison of $\tan \delta$ obtained from CG-MD and FEA simulations at varying temperatures. Markers with bolded borders indicate temperatures of $\tan \delta$ coincidence where comparisons are made (dashed line) – for instance, 407 K FEA and 450 K MD. (B) Stress and (C) strain field plots obtained from FEA indentation simulations on viscoelastic PMMA at temperatures specified in (A) using $d \sim 5 \text{ nm}$ and $R = 20 \text{ nm}$ (see SI for model details).

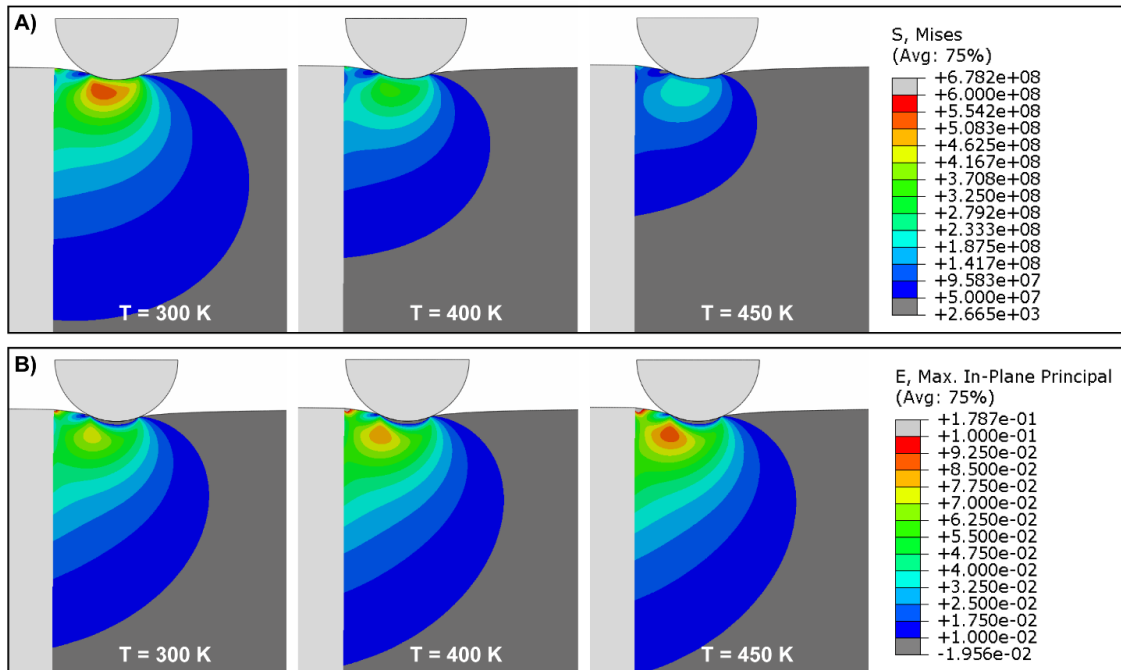


Figure S4. Von Mises stress and strain fields obtained from FEA indentation simulations on PMMA using a purely elastic model. The FEA model used for the simulations of elastic material behaviour were identical to the models built for FEA examination of viscoelastic behaviour with the exception of the material model used to describe the PMMA region. To approximate the elastic modulus at each temperature, the storage modulus was extracted from the experimental frequency dependent data at 300K, 400K and 450K for a fixed frequency of $\sim 2.5\text{Hz}$

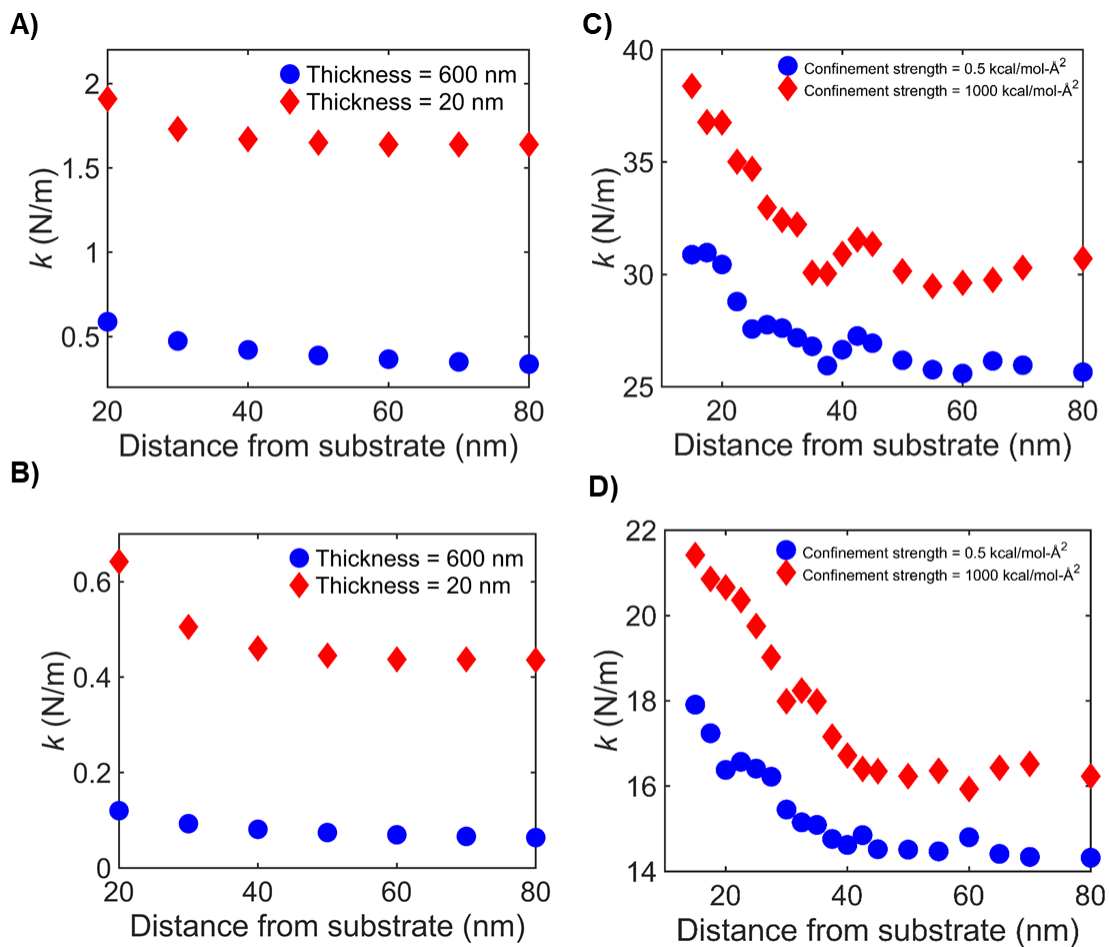


Figure S5. High-confinement films show dramatically higher absolute stiffness values compared to low-confinement films due to the bottom substrate. Absolute stiffness values obtained from indentation sweeps on the FEA Prony series model at (A) $T = 392$ K and (B) $T = 407$ K, and on the MD model at (C) $T = 300$ K and (D) $T = 400$ K.

5. References

1. Chung, P. C.; Glynos, E.; Green, P. F., The Elastic Mechanical Response of Supported Thin Polymer Films. *Langmuir* **2014**, *30* (50), 15200-15205.
2. Chung, P. C.; Green, P. F., The elastic mechanical response of nanoscale thin films of miscible polymer/polymer blends. *Macromolecules* **2015**, *48* (12), 3991-3996.
3. Chung, P. C.; Glynos, E.; Sakellariou, G.; Green, P. F., Elastic Mechanical Response of Thin Supported Star-Shaped Polymer Films. *ACS Macro Letters* **2016**, *5* (4), 439-443.
4. Xia, W. J.; Song, J. K.; Hsu, D. D.; Keten, S., Understanding the Interfacial Mechanical Response of Nanoscale Polymer Thin Films Via Nanoindentation. *Macromolecules* **2016**, *49* (10), 3810-3817.
5. Hsu, D. D.; Xia, W.; Arturo, S. G.; Keten, S., Systematic method for thermomechanically consistent coarse-graining: a universal model for methacrylate-based polymers. *Journal of chemical theory and computation* **2014**, *10* (6), 2514-2527.